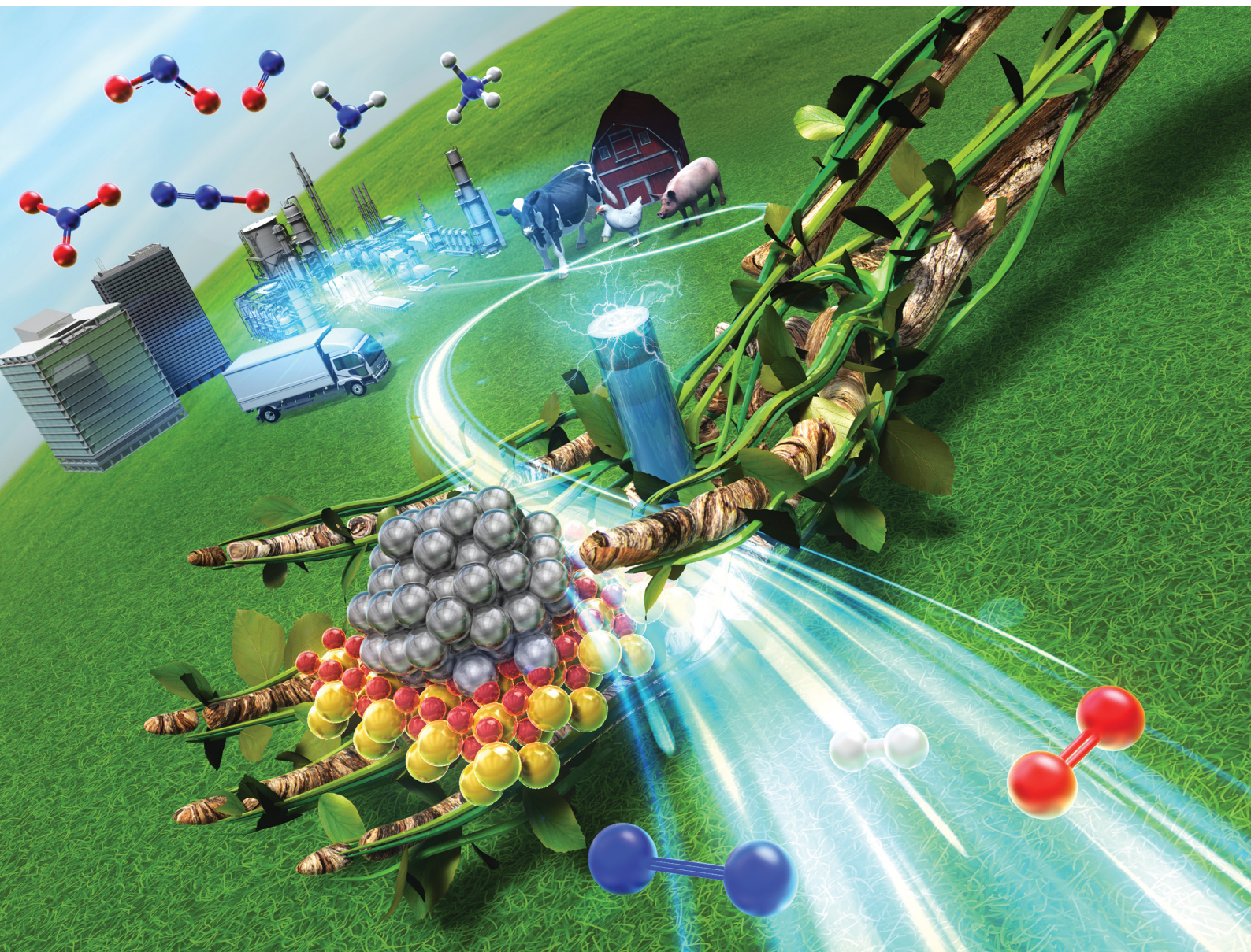


# ChemComm

Chemical Communications

[rsc.li/chemcomm](http://rsc.li/chemcomm)



ISSN 1359-7345

**FEATURE ARTICLE**

Ayaka Shigemoto and Yasushi Sekine  
Recent advances in low-temperature nitrogen oxide  
reduction: effects of electric field application



Cite this: *Chem. Commun.*, 2025, 61, 1559

## Recent advances in low-temperature nitrogen oxide reduction: effects of electric field application

Ayaka Shigemoto \* and Yasushi Sekine \*

This article presents a review of catalytic processes used at low temperatures to reduce emissions of nitrogen oxides (NO<sub>x</sub>) and nitrous oxide (N<sub>2</sub>O), which are exceedingly important in terms of their environmental impacts on the Earth. With conventional purification technologies, it has been difficult to remove these compounds under low-temperature conditions. By applying a catalytic process in an electric field for the three reactions of three-way catalysts (TWC), NO<sub>x</sub> storage reduction catalysts (NSR), and direct decomposition of N<sub>2</sub>O, we have achieved high catalytic activity even at low temperatures. By promoting ion migration on the catalyst surface, we have filled in the gaps in conventional catalytic technology and have opened the way to more efficient conversion of NO<sub>x</sub> and N<sub>2</sub>O.

Received 30th September 2024,  
Accepted 4th December 2024

DOI: 10.1039/d4cc05135a

rsc.li/chemcomm

### 1. Introduction

“Planetary boundaries” proposed by Rockström *et al.* in 2009 define the limits for maintaining the stability of the natural environment and ecosystems of the Earth. They constitute a guideline for evaluating the effects of human activities on the Earth system.<sup>1</sup> The “planetary boundaries” include nine items: climate change, loss of biodiversity, land use change, nitrogen and phosphorus cycles and so on. Human society can develop and prosper if activities remain within safe limits. However, if the limits are exceeded, irreversible environmental changes might occur for humanity and for the Earth. In 2023,

Richardson *et al.* reported that six of these nine items had already exceeded their respective danger zones.<sup>2</sup>

The nitrogen cycle represents the most severe of the problems, exceeding the limit by three times or more. Nitrogen, an essential element that maintains the balance of nature, circulates in various forms. For instance, nitrogen exists in the atmosphere as nitrogen molecules, N<sub>2</sub>, and also exists on Earth in compounds such as ammonia (NH<sub>3</sub>), nitrous acid (NO<sub>2</sub><sup>-</sup>), nitric acid (NO<sub>3</sub><sup>-</sup>), nitric oxide (NO), and nitrogen dioxide (NO<sub>2</sub>).<sup>3,4</sup> These nitrogen compounds are involved in a myriad of environmental difficulties such as air pollution, water pollution, climate change, stratospheric ozone depletion, eutrophication and acidification (Fig. 1).<sup>5,6</sup> In particular, the impacts of human activities on this nitrogen cycle are strongly significant. The following three issues are of crucial importance.

Waseda University, 3-4-1, Okubo, Shinjuku, Tokyo 1698555, Japan.  
E-mail: ayaka.shigemoto@nifty.com, ysekine@waseda.jp



**Ayaka Shigemoto**

*Ayaka Shigemoto received her BS, MS and PhD degrees from Waseda University, Japan, under the supervision of Prof. Yasushi Sekine. She is currently serving as a research associate at Waseda University. Her research interests include environmental catalysis, with a particular focus on the low-temperature catalytic conversion of nitrogen oxides under an electric field, which formed the core of her doctoral thesis.*



**Yasushi Sekine**

*Yasushi Sekine (b. 1968) obtained a PhD from the University of Tokyo in 1998 and became a professor in the Department of Applied Chemistry at Waseda University in 2012. He works with low temperature catalysis, specialising in protons and protonic transport in oxides and on their surfaces. Professor Sekine has published 235 journal papers, supervised 112 Master and 15 PhD students, and is a fellow of the RSC (FRSC) and a member of other national academies.*



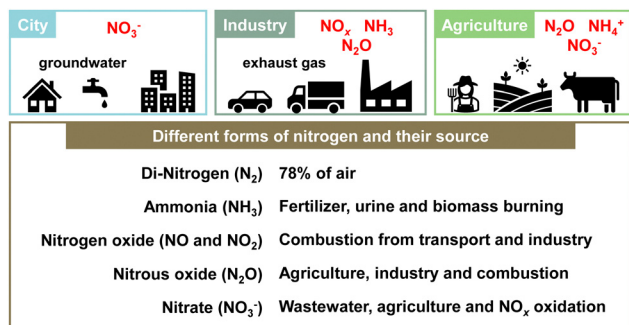


Fig. 1 Different forms of nitrogen in the environment.

The first is that the amount of ammonia supplied to human society by the Haber–Bosch process is enormous. It is necessary to consider its balance with nature. Of course, the Haber–Bosch process has improved the production of nitrogen fertilisers dramatically. Since the 20th century, it has greatly supported the improvement of agricultural productivity. However, at present, the contribution of natural nitrogen fixation is far outweighed by chemical fertilisers and other artificial sources of fixed nitrogen, which ultimately engender environmental degradation of the soil and hydrosphere.<sup>3</sup> Of the nitrogen fertiliser applied to agriculture, the nitrogen not absorbed by crops flows into rivers and the atmosphere, exacerbating a chain reaction of the diffusion of nitrogen compounds. This burden engenders excessive nitrogen loads on soil and water, causing eutrophication and groundwater pollution.

The second is the production of nitrogen oxides (NO<sub>x</sub>) through fuel combustion with air at high temperatures.<sup>7,8</sup> NO<sub>x</sub> produced by vehicles and industrial activities affects the human body, causing air pollution, acid rain, and harming forest and lake ecosystems. In fact, NO<sub>x</sub> is known to be produced in three ways: thermal NO<sub>x</sub>, which is produced by the reaction of nitrogen and oxygen in the air during high-temperature combustion; fuel NO<sub>x</sub>, which is produced by the oxidation of nitrogen in fuel; and prompt NO<sub>x</sub>, which is produced when natural gas is burned. Moreover, NO<sub>x</sub> is known to be emitted from systems of two types: (1) stationary sources such as gas engines, boilers, turbines, and chemical plants; and (2) mobile sources such as car and ship engines. As a NO<sub>x</sub> reduction technology, the selective catalytic reduction method has been put to practical use for stationary sources. Additionally, the three-way catalyst method has been used for mobile sources such as gasoline-powered cars. To a certain degree, many difficulties have been overcome. Nevertheless, technical issues remain to be solved in relation to reducing and controlling NO<sub>x</sub> emissions from catalysts in low-temperature environments, such as those encountered with hybrid vehicles.

The third category is emissions of N<sub>2</sub>O produced by agriculture and sewage treatment and during the denitrification process. Even with the development of technologies for removing NO<sub>x</sub> and NH<sub>3</sub>, one nitrogen compound that cannot be completely alleviated completely is N<sub>2</sub>O. In fact, N<sub>2</sub>O has a global warming effect about 300 times greater per molecule than carbon dioxide (CO<sub>2</sub>). In addition to being an ozone-depleting substance, it also

has a very long atmospheric lifetime of about 116 years.<sup>9</sup> It can be reasonably inferred that the amount of N<sub>2</sub>O produced from natural sources is more remarkable in quantity than that produced from human sources. Of these, it is thought that the primary sources of anthropogenic emissions are agricultural production and sewage treatment, but N<sub>2</sub>O is also produced during the denitrification process in the post-treatment stage of high-temperature combustion boilers for fossil fuels and automobile exhaust gas. Concerns have arisen about the impact of N<sub>2</sub>O on climate change, but N<sub>2</sub>O reduction technology development is being pursued.

As described above, from the perspective of planetary boundaries, the nitrogen cycle is a fundamentally important environmental issue. To address it and related issues, technological innovation and the introduction of new policies are necessary. Comprehensive efforts at creating a sustainable society must be undertaken. This paper summarises recent NO<sub>x</sub> and N<sub>2</sub>O catalytic conversion processes, technologies, and catalyst materials. Furthermore, we introduce our related efforts, specifically in developing electric field-assisted catalytic processes. The catalytic process of applying a direct current electric field to a semi-conductive catalyst is recognized for its ability to function at low temperatures and with high energy efficiency, making it a promising approach in the realm of sustainable catalytic technologies.

## 2. Nitrogen budget and wastewater treatment

The excessive production of NH<sub>3</sub> via the Haber–Bosch process has disrupted the nitrogen balance, leading to an overaccumulation of nitrogen in soils and aquatic systems. The nitrogen budget represents the equilibrium between the inputs and outputs of fixed nitrogen within a system. By calculating each nitrogen flux, the nitrogen budget provides insight into nitrogen pollution and the underlying nitrogen flows contributing to it. Recently, Hayashi and colleagues investigated nitrogen budgets in Japan during 2000–2015, eventually summarising nitrogen emissions to the atmosphere and aquatic environments.<sup>10</sup> Their findings indicate that of 5.76 million tons of nitrogen waste in 2010, 1.96 million tons of reactive nitrogen were released into the environment, with 64% emitted to the atmosphere and 36% to water bodies. Additionally, Zhang *et al.* compiled estimates of global nitrogen reservoirs.<sup>11</sup> The largest nitrogen reservoir on the Earth's surface is atmospheric N<sub>2</sub> gas (approximately 4 × 10<sup>9</sup> Tg N), followed by oceanic N<sub>2</sub> at 6.6 × 10<sup>5</sup> Tg N, terrestrial water (lakes, rivers, and groundwater) at 1.0 × 10<sup>4</sup> Tg N, and soils and coastal sediments at 1.1 × 10<sup>5</sup> Tg N. A large quantity of the fixed nitrogen in the environment is stored in oceans, with nitrate (NO<sub>3</sub><sup>-</sup>) being the most abundant form. The influx of large amounts of nitrogen compounds into water bodies, such as rivers and oceans, contributes to the eutrophication of marine environments.

In response to these circumstances, the conversion of NO<sub>3</sub><sup>-</sup> in industrial and agricultural wastewater,<sup>12</sup> adsorption techniques for selective removal of nitrate from water,<sup>13</sup> and many techniques for the removal of ammonia nitrogen from wastewater have been



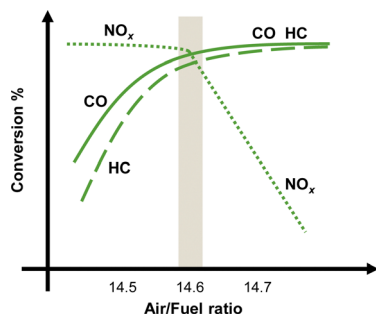


Fig. 2 Typical three-way catalyst performance as a function of the air-fuel ratio.

developed and investigated. Xiang *et al.* compared various ammonia-nitrogen wastewater treatment methods: physical (*e.g.*, air stripping, membrane technology), chemical (*e.g.*, struvite precipitation method, electrochemical oxidation and photocatalysis), and biological.<sup>14</sup> Among them, methods such as acid adsorption, struvite precipitation, membrane enrichment, microalgae and photosynthetic bacteria can recover ammonia nitrogen with satisfactory efficiency, which is expected to be more beneficial in terms of a circular economy and energy than merely removing it. In the future, based on the current main methods for ammonia-nitrogen recovery, improvements or combinations with other methods are expected to be effective for recovering ammonia nitrogen in more complex wastewater mixtures.

### 3. The NO<sub>x</sub> removal catalyst and system

Demonstrably, NO<sub>x</sub> causes environmental problems such as acid rain and photochemical smog, and poses risks to human health. Automobile exhaust emissions are regarded as one cause of air pollution. Exhaust gas regulations have been implemented.<sup>15</sup> The typical composition of exhaust emissions from gasoline engine vehicles under usual driving conditions is the following: carbon monoxide (CO < 0.5 vol%), unburned hydrocarbons (HC < 500 ppmv), nitrogen oxides (NO<sub>x</sub> < 1000 ppmv), water vapour (H<sub>2</sub>O: 10 vol%), carbon dioxide (CO<sub>2</sub>: 10 vol%), and oxygen (O<sub>2</sub> > 0.5 vol%).<sup>16</sup> Of these gases, HC, CO and NO<sub>x</sub> are the main harmful pollutants. Purification of these gases is necessary. Currently, a three-way catalyst (TWC) is used to convert CO, HC and NO<sub>x</sub> respectively into the harmless products of CO<sub>2</sub>, N<sub>2</sub> and H<sub>2</sub>O to control and suppress the environmental impacts of gasoline vehicle exhaust gas.<sup>17,18</sup> The design of a TWC consists of a monolith substrate, an oxygen storage promoter material with a high surface area, an active catalyst (platinum group metals or PGMs), and a promoter material. For the reaction over the TWC, the atmosphere is particularly important. Fig. 2 shows a graph with the air-fuel ratio on the horizontal axis and the purification rate of each component on the vertical axis.<sup>18</sup> When the air-fuel ratio is close to the stoichiometric point of approximately 14.6–14.7 (theoretical air-fuel ratio), the TWC functions efficiently. Simultaneous conversion of CO/HC/NO<sub>x</sub> is achieved. The side

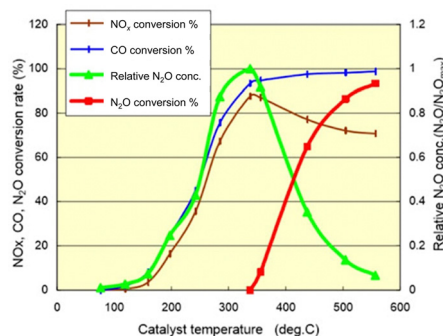


Fig. 3 Conversion of exhaust pollutant species over a TWC. Cited from National Traffic Safety and Environment Laboratory. Research on low emission vehicles: effect of catalyst temperature behaviour on nitrous oxide (N<sub>2</sub>O) emissions in cold climates.

with a value smaller than the theoretical air-fuel ratio is called a rich atmosphere. The other side with a value larger than the theoretical air-fuel ratio is called a lean atmosphere.

In catalytic reactions, an important factor for exhaust gas purification is the reaction temperature. Fig. 3 shows a graph with the gas temperature at the catalyst inlet (automobile exhaust gas temperature) on the horizontal axis and the purification rate of each component on the vertical axis.<sup>19</sup> Ensuring high purification performance requires raising of the catalyst inlet temperature to a certain extent: around 573 K or more. This fact can also be understood from the Arrhenius equation presented in Fig. 4. The Arrhenius equation is expressed as  $\ln k = \ln A - E_a/RT$ , where  $A$  denotes the frequency factor and  $E_a$  stands for the apparent activation energy. It has been proven by experimentation that plotting  $\ln k$  against  $1/T$  for many reactions produces a straight line, and that the reaction rate increases as the temperature rises. Based on the Arrhenius law, it is considered difficult to lower the temperature of the reaction. However, to overcome this challenge, research and development of catalytic processes for lowering the temperature have been progressing in recent years. Here, we categorise recent research trends into three categories: (1) the development of catalyst materials to lower the activation energy of reactions, (2) the development of processes to increase the reactant concentration for increasing reaction rates, and (3) the development of processes to increase the reaction rate constant by introducing external force fields.

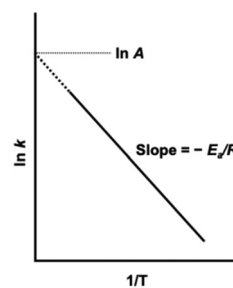


Fig. 4 The Arrhenius plot.









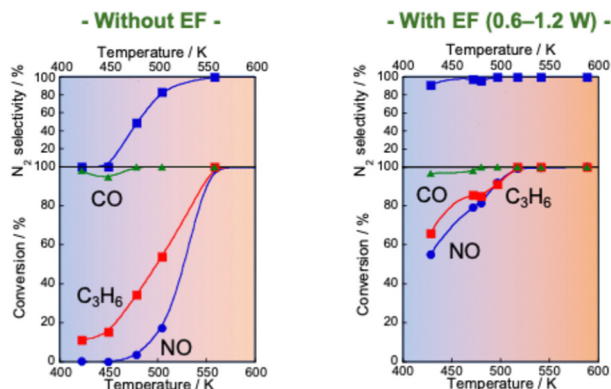


Fig. 7 NO, CO and C<sub>3</sub>H<sub>6</sub> conversion and N<sub>2</sub> selectivity over 0.5 wt% Pd/Ce<sub>0.7</sub>Zr<sub>0.3</sub>O<sub>2</sub> under NO–C<sub>3</sub>H<sub>6</sub>–CO–O<sub>2</sub>–H<sub>2</sub>O reaction: NO, 2500 ppm; C<sub>3</sub>H<sub>6</sub>, 500 ppm; CO, 3000 ppm; O<sub>2</sub>, 2500 ppm; H<sub>2</sub>O, 70 000 ppm; Ar balance; SV, 72 000 h<sup>-1</sup>, applying 1.5 mA direct current. Reproduced from ref. 75 with permission from RSC Publishing, copyright 2021.

### 3.4. Electric field-assisted three-way catalysis

Although EHC, plasma and microwave assistance constitute important technical solutions for the low-temperature activity of catalysts, they yet require large amounts of electrical energy. That energy presents important challenges for maintaining stable catalytic reactions.

In contrast, the catalytic process of applying a direct current electric field to a semi-conductive catalyst is known to be able to operate at low temperatures and to be energy efficient.<sup>72–74</sup> Various applications to different reactions have been investigated. Applying an electric field to the catalytic process of NO<sub>x</sub> conversion is also very attractive.

Reportedly, a Pd catalyst (Pd/Ce<sub>0.7</sub>Zr<sub>0.3</sub>O<sub>2</sub>) in an electric field shows extremely high three-way catalytic activity (TWC: NO–C<sub>3</sub>H<sub>6</sub>–CO–O<sub>2</sub>–H<sub>2</sub>O).<sup>75,76</sup> When an electric field is applied, the conversions of NO, C<sub>3</sub>H<sub>6</sub> and CO and the N<sub>2</sub> selectivity are extremely high, even with coexisting O<sub>2</sub> and H<sub>2</sub>O and even at low temperatures (423–473 K), as presented in Fig. 7. The NO conversion and N<sub>2</sub> selectivity were 54.9% and 91.3% respectively, in the presence of an electric field at 428 K. NO conversion reaches 100% at 517 K. In contrast, in the absence of an electric field, the NO conversion rate and N<sub>2</sub> selectivity are very low (almost 0%) in the low-temperature range. For these tests, the catalyst layer temperature was measured directly using a thermocouple attached to the catalyst. The Joule heat effect from the applied direct current on the catalytic activity was confirmed. As a result, it was possible to state that the high

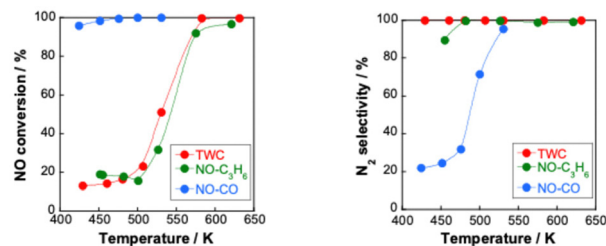


Fig. 8 NO conversion and N<sub>2</sub> selectivity over 0.5 wt% Pd/Ce<sub>0.7</sub>Zr<sub>0.3</sub>O<sub>2</sub> under NO–C<sub>3</sub>H<sub>6</sub>–CO–O<sub>2</sub>–H<sub>2</sub>O reaction (NO, 2500 ppm; C<sub>3</sub>H<sub>6</sub>, 500 ppm; CO, 3000 ppm; O<sub>2</sub>, 2500 ppm; H<sub>2</sub>O, 70 000 ppm; Ar balance; 200 cc min<sup>-1</sup> total flow); NO–CO–O<sub>2</sub>–H<sub>2</sub>O reaction (NO, 2500 ppm; CO, 3000 ppm; O<sub>2</sub>, 2500 ppm; H<sub>2</sub>O, 70 000 ppm; Ar balance; 200 cc min<sup>-1</sup> total flow) and NO–C<sub>3</sub>H<sub>6</sub>–O<sub>2</sub>–H<sub>2</sub>O reaction (NO, 2500 ppm; C<sub>3</sub>H<sub>6</sub>, 500 ppm; O<sub>2</sub>, 2500 ppm; H<sub>2</sub>O, 70 000 ppm; Ar balance; 200 cc min<sup>-1</sup> total flow) with and without an electric field at 3 mA (denoted as EF); reproduced from ref. 75 with permission from RSC Publishing, copyright 2021.

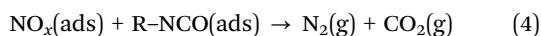
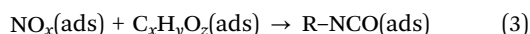
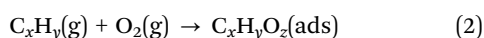
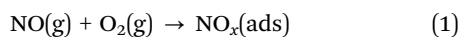
activity/selectivity was not attributable to Joule heat. Furthermore, the power consumption for applying the current was only 1.2 W at 428 K in this case. Therefore, catalysis in the electric field enables a highly efficient three-way catalytic system at much lower temperatures than those used for conventional systems. This promotion effect of the electric field differs entirely to that of EHC or plasma reactions introduced in the preceding section. To verify whether plasma effects can be neglected in this system, a plasma reaction was conducted using the same TWC gas composition. At 375 K and 468 K, the respective NO conversion rates achieved by plasma were only 5.6% and 7.4%. These values are markedly lower than the catalytic activity under an electric field shown in Table 1. Consequently, the promotion effect of the electric field on the TWC reaction is considerably greater than that of plasma reactions. The contribution of reducing agents (C<sub>3</sub>H<sub>6</sub> and CO) to catalytic NO reduction at low temperatures in the electric field was investigated. Fig. 8 shows the NO conversion rate with and without an electric field in the low-temperature range (420–500 K catalyst layer temperature). In the NO–CO–O<sub>2</sub>–H<sub>2</sub>O conditions, the NO conversion rate was almost 100%, irrespective of the presence or absence of an electric field. No significant difference was found in the NO conversion rate. In contrast, in the NO–C<sub>3</sub>H<sub>6</sub>–O<sub>2</sub>–H<sub>2</sub>O conditions, a clear difference was found in the NO conversion rate with or without an electric field at 420–500 K. Furthermore, the NO conversion rate and N<sub>2</sub> selectivity achieved when an electric field was applied under the NO–C<sub>3</sub>H<sub>6</sub>–O<sub>2</sub>–H<sub>2</sub>O conditions were almost identical as a result of the TWC conditions. These results suggest that the NO–C<sub>3</sub>H<sub>6</sub>

Table 1 NO conversion over 0.5 wt% Pd/Ce<sub>0.7</sub>Zr<sub>0.3</sub>O<sub>2</sub> under NO–C<sub>3</sub>H<sub>6</sub>–CO–O<sub>2</sub>–H<sub>2</sub>O reaction (NO, 2500 ppm; C<sub>3</sub>H<sub>6</sub>, 500 ppm; CO, 3000 ppm; O<sub>2</sub>, 2500 ppm; H<sub>2</sub>O, 7 vol%, Ar balance; 200 cc min<sup>-1</sup> total flow) for various reactions. Reproduced from ref. 75 with permission from RSC Publishing, copyright 2021

	NO conversion/%		
Plasma reaction	5.6 (at 375 K)	7.4 (at 468 K)	
NO decomposition in the electric field	2.7 (at 451 K)	2.3 (at 532 K)	2.5 (at 625 K)
Heated catalytic reaction	0.0 (at 420 K)	0.3 (at 449 K)	0.26 (at 478 K)
Electric field reaction with reductants (3 mA)	19.1 (at 414 K)	16.5 (at 433 K)	20.5 (at 457 K)



reaction is dominant under the TWC conditions with an electric field at low temperatures (420–500 K). To clarify the effects of coexisting O<sub>2</sub> on the TWC reaction, we conducted O<sub>2</sub> partial pressure dependence tests under both NO–CO–O<sub>2</sub>–H<sub>2</sub>O and NO–C<sub>3</sub>H<sub>6</sub>–O<sub>2</sub>–H<sub>2</sub>O conditions with and without an electric field. Under the NO–CO–O<sub>2</sub>–H<sub>2</sub>O conditions, the conversion rate behaviours of the NO, CO, and O<sub>2</sub> in response to changes in O<sub>2</sub> concentration were the same with and without an electric field. The NO conversion rate decreased and the CO conversion rate increased concomitantly with increasing O<sub>2</sub> concentration. These trends suggest that CO was consumed by the CO–O<sub>2</sub> reaction rather than by the NO–CO reaction. These findings indicate that the electric field does not contribute to the NO–CO and CO–O<sub>2</sub> reactions in the low-temperature region (420–500 K). In contrast, under NO–C<sub>3</sub>H<sub>6</sub>–O<sub>2</sub>–H<sub>2</sub>O conditions, a drastic difference was found in the dependence of the NO reaction rate on the O<sub>2</sub> concentration with and without an electric field. In the absence of an electric field, the NO reaction rate shows negative dependence on the O<sub>2</sub> concentration. However, under electric field conditions, the NO reaction rate is positively correlated with the O<sub>2</sub> concentration at 0–1000 ppm. The NO reaction rate decreases considerably at O<sub>2</sub> concentrations of 1000–1500 ppm because O<sub>2</sub> causes excessive adsorption on the Pd metal, the active site of the NO–C<sub>3</sub>H<sub>6</sub> reaction. By contrast, O<sub>2</sub> positively affects the NO–C<sub>3</sub>H<sub>6</sub> reaction at 0–1000 ppm O<sub>2</sub>. Reportedly, NO<sub>x</sub> is reduced by hydrocarbons according to eqn (1)–(4).<sup>77</sup> The partially oxidised species of hydrocarbons (C<sub>x</sub>H<sub>y</sub>O<sub>z</sub>) are known to be important intermediates in HC-SCR.<sup>78</sup>



To investigate the adsorbed species and surface reactions on the Pd/Ce<sub>0.7</sub>Zr<sub>0.3</sub>O<sub>2</sub> catalyst, *in situ* DRIFTS measurements were taken by switching from C<sub>3</sub>H<sub>6</sub> to NO flow. The results presented in Fig. 9 indicate that NO is adsorbed onto the Pd/Ce<sub>0.7</sub>Zr<sub>0.3</sub>O<sub>2</sub> catalyst as NO<sub>2</sub><sup>-</sup>/NO<sub>3</sub><sup>-</sup>. At the same time, adsorbed C<sub>3</sub>H<sub>6</sub> is oxidised by the surface lattice oxygen of the support to form an

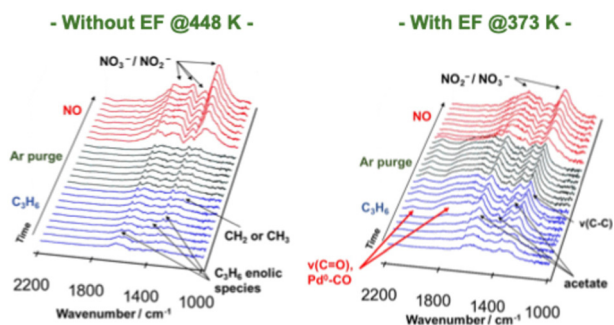


Fig. 9 DRIFT spectra of Pd/Ce<sub>0.7</sub>Zr<sub>0.3</sub>O<sub>2</sub> during the transient test, switching from C<sub>3</sub>H<sub>6</sub> to NO flow. Reproduced from ref. 76 with permission from RSC Publishing, copyright 2022.

oxygenated species (C<sub>x</sub>H<sub>y</sub>O<sub>z</sub>). Next, NO<sub>2</sub><sup>-</sup>/NO<sub>3</sub><sup>-</sup> and C<sub>x</sub>H<sub>y</sub>O<sub>z</sub> species mutually react to produce N<sub>2</sub>, CO<sub>2</sub> and H<sub>2</sub>O as the final products. However, without an electric field, NO and C<sub>3</sub>H<sub>6</sub> are simply adsorbed onto the catalyst surface; then NO reduction by C<sub>3</sub>H<sub>6</sub> does not proceed. Therefore, in TWC under an electric field at low temperatures, promoting partial oxidation of C<sub>3</sub>H<sub>6</sub> using the surface lattice oxygen of the catalyst support is an important role of the electric field. This promotion allows high activity of the NO–C<sub>3</sub>H<sub>6</sub> reaction to be achieved even at low temperatures. Although the low-temperature activity is still insufficient, designing catalysts based on the mechanism of the electric field-assisted TWC reaction can engender a more power-efficient process with enhanced low-temperature activity. For example, because application of the electric field promotes the release of surface lattice oxygen on the catalyst support, adding a redox-active metal to improve oxygen release might be effective.

### 3.5. Electric field-assisted NSR process for lean NO<sub>x</sub> reduction

Although NSR systems have been developed to purify exhaust gases from lean-burn engines, such systems require periodic operation, which adversely affects fuel efficiency.<sup>46,47</sup> As a novel approach to this difficulty, catalysis in an electric field was proposed for lean NO<sub>x</sub> reduction.<sup>79</sup> This new NSR process uses H<sub>2</sub> in a lean atmosphere to reduce stored NO<sub>x</sub> without switching to rich combustion after NO<sub>x</sub> storage, thereby improving engine efficiency. Lean NO<sub>x</sub> reduction tests were conducted with and without an electric field using a 3 wt% Pt–16 wt% BaO/CeO catalyst. Total flow of 200 cc min<sup>-1</sup> of 0.2 vol% H<sub>2</sub>, 8 vol% O<sub>2</sub> and 10 vol% H<sub>2</sub>O was supplied. The stored NO<sub>x</sub> was reduced at 423 K for 1 h. The results are presented in Fig. 10. In the absence of an electric field, the conversion rate from NO<sub>x</sub> to N<sub>2</sub> was only 2.9%. By contrast, when a 6 mA electric field was applied, a high conversion rate of 13.1% was obtained even under lean conditions at the low temperature of 423 K. The conversion of adsorbed NO<sub>x</sub> to N<sub>2</sub> increased linearly over time. This reaction behaviour remained almost unchanged even when the time of electric field application was doubled. The conversion rate more than doubled: from 13.1% to 29.1%. Observation of surface-adsorbed species by *in situ* transmission infrared spectroscopy (TIRS) measurements confirmed that more nitrate species were removed from the surface when an

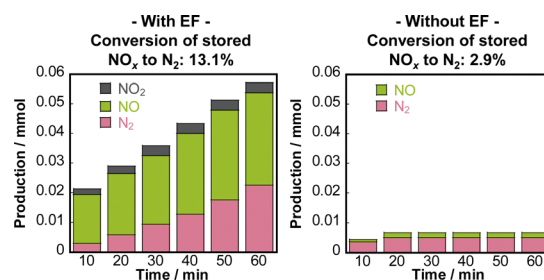


Fig. 10 Conversion of stored NO<sub>x</sub> to N<sub>2</sub>, and the distribution of nitrogen-containing species in the outlet gas, calculated as nitrogen-based. Reproduced from ref. 79 with permission from RSC Publishing, copyright 2024.



electric field was applied in a lean atmosphere. The breakdown of the H<sub>2</sub> consumption during the reduction of NO<sub>x</sub> adsorbed onto the Ba site to N<sub>2</sub> and NO was calculated from the stoichiometric ratios of H<sub>2</sub>, N<sub>2</sub>, and NO.<sup>80–82</sup> The findings indicate that the total consumption of H<sub>2</sub> used to produce N<sub>2</sub> and NO in the electric field was 0.102 mmol, which is almost equal to the extra H<sub>2</sub> consumed during the application of the electric field (0.107 mmol). These findings suggest that the 3 wt% Pt–16 wt% BaO/CeO<sub>2</sub> catalyst can convert the adsorbed NO<sub>x</sub> to N<sub>2</sub> using H<sub>2</sub>, even in a lean atmosphere, by application of an electric field. The important role of the electric field in NO<sub>x</sub> reduction is to promote the activation and migration of hydrogen species. Earlier studies have demonstrated that applying an electric field to the reaction promotes hydrogen migration on the surface of the support.<sup>74,83–85</sup> In heterogeneous catalysts under the electric field, the proton conductivity on the catalyst surface plays an important role: it provides a reaction pathway by collision between H<sup>+</sup> on the catalyst support and adsorbed substances on the supported metal.

To elucidate the promotion of hydrogen migration by the application of the electric field, lean NO<sub>x</sub> reduction tests were conducted using a physical mixture of 3 wt% Pt/CeO<sub>2</sub> and 16 wt% Ba(NO<sub>3</sub>)<sub>2</sub>/CeO<sub>2</sub> catalysts. In this physical mixture catalyst, Pt and Ba(NO<sub>3</sub>)<sub>2</sub>, which is pre-loaded with nitrate, are present separately. The results demonstrated that nitrate decomposition occurs not only near Pt but also at locations distant from Pt during the application of the electric field. In the lean NO<sub>x</sub> reduction in the electric field, NO<sub>x</sub> reduction proceeded only slightly without hydrogen, indicating that NO<sub>x</sub> reduction results from hydrogen migration because of the electric field application. Furthermore, to assess the role of Pt for hydrogen migration, NO<sub>x</sub> reduction tests were conducted using only the 16 wt% Ba(NO<sub>3</sub>)<sub>2</sub>/CeO<sub>2</sub> catalyst without Pt in an electric field. The amount of reduced NO<sub>x</sub> decreased without Pt, indicating that Pt is necessary for hydrogen migration in an electric field. Therefore, hydrogen migrates from the Pt site to the adsorbed nitrate during lean NO<sub>x</sub> reduction and reacts with the nitrate directly. Finally, based on the conventional mechanism of H<sub>2</sub>-induced NSR reactions (Section 3.2 presents related details), the EF-assisted NSR mechanism can be characterised as follows: during lean NO<sub>x</sub> reduction, hydrogen is migrated from the Pt site to the Ba(NO<sub>3</sub>)<sub>2</sub>; it then reacts with the nitrate directly. The released NO<sub>x</sub> reaches the Pt site, where the NO<sub>x</sub> is

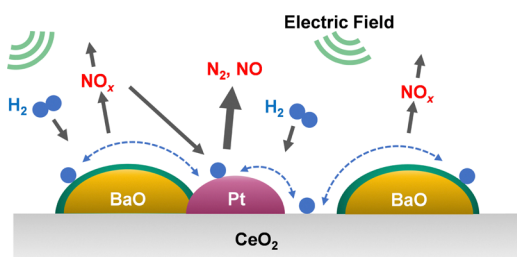


Fig. 11 Assumed reaction model for electric field-assisted lean NO<sub>x</sub> reduction over 3 wt% Pt–16 wt% BaO/CeO<sub>2</sub>. Reproduced from ref. 79 with permission from RSC Publishing, copyright 2024.

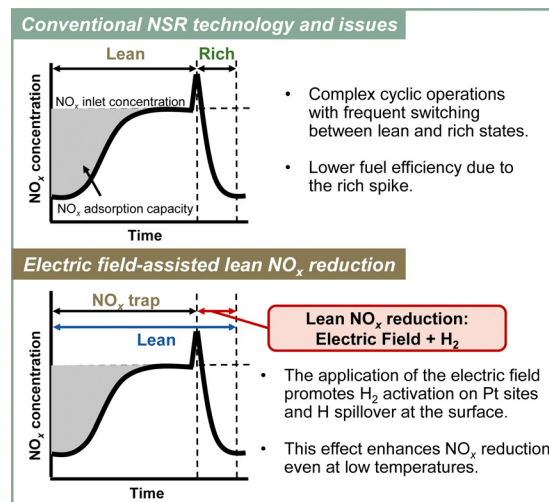
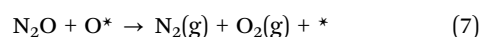
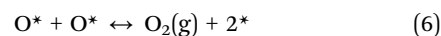
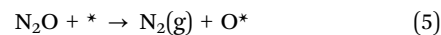


Fig. 12 Conceptual diagram of the electric field-assisted catalytic process approach to the issues of conventional NSR technology.

reduced to form N<sub>2</sub> (Fig. 11). This proposed EF-assisted NSR process can reduce stored NO<sub>x</sub> under excess oxygen conditions and at low temperatures. However, it currently has limitations attributable to insufficient activity and extended reduction times (e.g., even after one hour of reduction, NO<sub>x</sub> conversion at 423 K remains at 13.1%). To overcome these shortcomings, it will be necessary to design catalysts with closer Pt and BaO contact and to optimise the applied current. For future applications, this innovative method is expected to use surplus vehicle power to purify exhaust gas, promote hydrogen transfer, and improve NO<sub>x</sub> reduction, even at low temperatures (Fig. 12).

## 4. N<sub>2</sub>O removal

During both nitrification and denitrification processes, N<sub>2</sub>O is produced by various microorganisms through the oxidation and reduction of nitrogen. Mainly, N<sub>2</sub>O of natural origin is produced during the processes of nitrification and denitrification occurring in the oceans and soil. The main sources of anthropogenic N<sub>2</sub>O emissions are agriculture, engine exhaust gas, and emissions from nitric acid plants.<sup>9,86</sup> The most suitable post-treatment technologies used for N<sub>2</sub>O reduction are direct catalytic cracking and selective catalytic reduction (SCR).<sup>86–88</sup> Direct decomposition is the most efficient, cost-effective and environmentally friendly method for reducing N<sub>2</sub>O emissions. It is a process by which N<sub>2</sub>O is decomposed directly into non-toxic and harmless N<sub>2</sub> and O<sub>2</sub> on a catalyst, creating no secondary pollution. The reaction temperature can be lower than that of pyrolysis.<sup>86</sup> The widely accepted model for the reaction mechanism of direct catalytic decomposition of N<sub>2</sub>O consists of the following three basic reaction equations.<sup>89–92</sup>



The  $\text{N}_2\text{O}$  molecule is adsorbed onto the active site (\*) on the catalyst surface. It then decomposes into  $\text{N}_2(\text{g})$  and adsorbed oxygen (reaction (5)). Subsequently, the active site is regenerated by the Langmuir–Hinshelwood (L–H) and/or Eley–Rideal (E–R) mechanisms. Thereby, the entire catalytic cycle is completed. In other words, the catalytic surface is regenerated by recombination of adsorbed oxygen species (reaction (6): L–H mechanism) or reaction with another  $\text{N}_2\text{O}$  molecule (reaction (7): E–R mechanism). It is noteworthy that while the recombination of oxygen atoms is a reversible process, regeneration of the active site by  $\text{N}_2\text{O}$  is irreversible because  $\text{N}_2\text{O}$  and  $\text{O}_2$  adsorb on the catalyst, mutually competing.<sup>93,94</sup> Adding reducing agents ( $\text{NO}$ ,<sup>95</sup>  $\text{NH}_3$ ,<sup>96</sup>  $\text{H}_2$ ,<sup>97</sup>  $\text{CO}$ ,<sup>98</sup>  $\text{CH}_4$ ,<sup>99</sup>  $\text{C}_3\text{H}_6$ ,<sup>100</sup>) is known to lower the reaction temperature of catalytic reduction of  $\text{N}_2\text{O}$  and to improve catalytic efficiency. Although the operational cost of SCR might increase because of the consumption of a certain amount of reducing agent, the removal of  $\text{N}_2\text{O}$  is thought to be accelerated by more easily removing surface oxygen in the presence of a reducing agent.<sup>86</sup>

#### 4.1. Synergistic catalytic processes of $\text{N}_2\text{O}$ removal

Wu *et al.* outlined  $\text{N}_2\text{O}$  conversion technologies systematically using not only conventional thermal catalysis, but also light, electricity, and non-catalytic methods. Improvement of  $\text{N}_2\text{O}$  decomposition performance by coupling technologies such as plasma synergistic catalysis and microwave-assisted catalysis has been demonstrated.<sup>88</sup> In addition, Vadikkeetil *et al.* introduced the salient benefits of plasma–catalyst hybrid methods, which are applied widely to  $\text{N}_2\text{O}$  decomposition, including the abilities to initiate chemical reactions at low temperatures and to improve selectivity.<sup>101</sup> In most cases, a single-stage plasma catalytic reactor is used, in which the catalyst pellets are in direct contact with the alternating current (AC)-driven plasma.<sup>102,103</sup> The synergistic effect of NTP (non-thermal plasma) on  $\text{N}_2\text{O}$  catalytic decomposition with hydroxyapatite (HAP)-supported Rh and Fe catalysts was studied by Tan *et al.*<sup>102</sup> When NTP is applied, the  $\text{N}_2\text{O}$  conversion rate of RhFe/HAP-11 at 473 K increases considerably from 7.1% to 90.0%. This improvement is attributable to the involvement of free radicals in the discharge process, and to the longer lifetime of active species, even at high temperatures. The reaction using NTP technology alone requires great amounts of energy. For example, the denitrification efficiency is only 46.6% at an output power of 2 kW. By contrast, NTP combined with RhFe/HAP catalysts can achieve denitrification efficiency of 90% for 10 vol%  $\text{N}_2\text{O}$  using plasma output energy of only 4 W and a reaction temperature of 473 K. Jo *et al.* and Ko *et al.* have reported  $\gamma\text{-Al}_2\text{O}_3$  as effective for  $\text{N}_2\text{O}$  decomposition using the plasma catalytic process.<sup>103,104</sup> Among the metals investigated (Ru, Co, Cu, V, *etc.*), Ru was found to be the most suitable catalyst for  $\text{N}_2\text{O}$  decomposition in the plasma catalytic reactor.<sup>103</sup> In the absence of plasma, the decomposition efficiency decreased considerably from 59% to 9% as the oxygen content was changed from 0% to 20%. Similarly, the plasma–catalyst decomposition efficiency decreased concomitantly with increasing  $\text{O}_2$  content, but the degree of decrease was not as pronounced as in the case of using the catalyst alone (from 90% to about 65%). In addition, Li *et al.* summarised the  $\text{N}_2\text{O}$  decomposition mechanism.<sup>104</sup>

Microwave-assisted  $\text{N}_2\text{O}$  decomposition was investigated using an alumina-modified nickel–cobalt-based SiC (NiCoAl/SiC).<sup>105</sup> For this study, research was conducted of high concentrations of  $\text{N}_2\text{O}$  (20 vol%–50 vol%  $\text{N}_2\text{O}$ ) to mimic the typical composition of the downstream from an adipic acid production plant. The results clarified that the microwave-assisted process removed  $\text{N}_2\text{O}$  completely from the high-concentration stream (50 vol%) at 823 K. In actuality, this is the same temperature necessary to remove  $\text{N}_2\text{O}$  from a low-concentration gas stream (20 vol%) using conventional heating processes. Microwave heating technology allows selective heating of the catalyst. The heat flux is directed from the inside to the outside of the catalyst bed, which is the opposite of conventional heating, thereby minimising energy losses and creating a more uniform temperature profile within the catalyst bed. As a result, better catalyst performance and shorter processing times can be achieved.<sup>106</sup> Furthermore, because microwave heating is an electricity-based technology, some room remains for the electrification of industrial processes, which is thought to enhance environmental sustainability.

#### 4.2. Catalytic $\text{N}_2\text{O}$ decomposition in the presence of $\text{O}_2$ with an electric field

We have developed a process combining an electric field catalytic process with  $\text{N}_2\text{O}$  decomposition reactions, which establishes an  $\text{N}_2\text{O}$  direct decomposition cycle at low temperatures.<sup>107</sup> Results have shown that applying an electric field to a 0.5 wt% Rh/Ce<sub>0.7</sub>Zr<sub>0.3</sub>O<sub>2</sub> catalyst enables efficient decomposition of  $\text{N}_2\text{O}$ , even at low temperatures and in the presence of excess oxygen and water vapour (Fig. 13).

Furthermore, the results indicate that the reaction is accelerated when assisted by an electric field, even when using inexpensive base metals such as Fe, Co, Ni, or Cu. Moreover, the reaction can be driven with extremely low energy consumption, requiring power consumption of only around 0.6 W. To elucidate the mechanism of direct decomposition of  $\text{N}_2\text{O}$ , we conducted tests to measure the effect of partial pressures of  $\text{N}_2\text{O}$  and  $\text{O}_2$ . The relevant results are presented in Table 2.

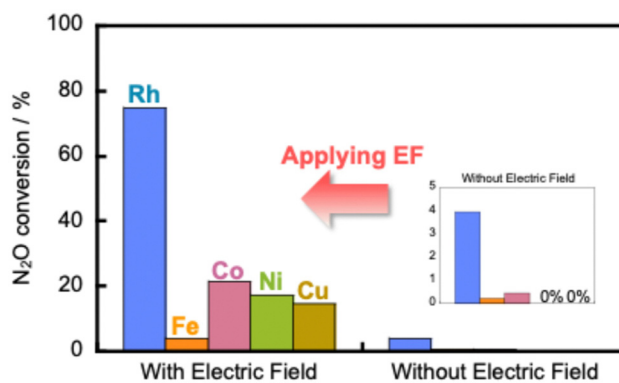


Fig. 13 Catalytic decomposition of  $\text{N}_2\text{O}$  over 0.5 wt% Rh/Ce<sub>0.7</sub>Zr<sub>0.3</sub>O<sub>2</sub> and 5 wt% Fe, Co, Ni, Cu/Ce<sub>0.7</sub>Zr<sub>0.3</sub>O<sub>2</sub> catalysts with and without the electric field at 473 K. Conditions: 1000 ppm  $\text{N}_2\text{O}$  + 10%  $\text{O}_2$ ; 200 mg catalyst weight; 100 mL min<sup>-1</sup> total flow rate; SV, 50 000 h<sup>-1</sup>; 0 or 6 mA current. Reproduced from ref. 107 with permission from RSC Publishing, copyright 2024.







addition, technologies for controlling N<sub>2</sub>O emissions from agriculture and sewage treatment are being earnestly sought. There is ongoing development of materials that adsorb low-concentration N<sub>2</sub>O. In the future, it will also be fundamentally important to develop a technology process for regenerating N<sub>2</sub>O adsorbents. Therefore, the combination of N<sub>2</sub>O adsorbents and electric-field-assisted catalysts appears to be promising. Important future prospects include improved low-cost, low-temperature catalysis, and development of new catalyst materials such as alloys or single-atom catalysts (SAC)/dual-atom-site catalysts (DACs), all while enhancing our understanding of energy-saving catalytic processes. Combining these technologies and concepts is hoped to engender the development of innovative exhaust gas purification catalysts. In addition, the collaboration of policy and technological innovation is expected to support the achievement of a more practical and sustainable nitrogen cycle. Further progress is also anticipated in NO<sub>x</sub> and N<sub>2</sub>O reduction technology.

## Author contributions

Data curation and formal analysis: A. Shigemoto, Y. Sekine, investigation: A. Shigemoto, methodology: A. Shigemoto, visualization: A. Shigemoto, writing – original draft, review & editing: A. Shigemoto, Y. Sekine, conceptualization, project administration and supervision: Y. Sekine.

## Data availability

The data supporting this article have been included in the manuscript itself and cited literature.

## Conflicts of interest

There are no conflicts to declare.

## Notes and references

- J. Rockström, W. Steffen, K. Noone, Å. Persson, F. S. Chapin, E. F. Lambin, T. M. Lenton, M. Scheffer, C. Folke, H. J. Schellnhuber, B. Nykvist, C. A. de Wit, T. Hughes, S. van der Leeuw, H. Rodhe, S. Sörlin, P. K. Snyder, R. Costanza, U. Svedin, M. Falkenmark, L. Karlberg, R. W. Corell, V. J. Fabry, J. Hansen, B. Walker, D. Liverman, K. Richardson, P. Crutzen and J. A. Foley, *Nature*, 2009, **461**, 472–475.
- K. Richardson, W. Steffen, W. Lucht, J. Bendtsen, S. E. Cornell, J. F. Donges, M. Drüke, I. Fetzer, G. Bala, W. von Bloh, G. Feulner, S. Fiedler, D. Gerten, T. Gleeson, M. Hofmann, W. Huiskamp, M. Kummu, C. Mohan, D. Nogués-Bravo, S. Petri, M. Porkka, S. Rahmstorf, S. Schaphoff, K. Thonicke, A. Tobian, V. Virkki, L. Wang-Erlandsson, L. Weber and J. Rockström, *Sci. Adv.*, 2023, **9**, eadh2458.
- L. Y. Stein and M. G. Klotz, *Curr. Biol.*, 2016, **26**, R94–R98.
- S. Reis, M. Bekunda, C. M. Howard, N. Karanja, W. Winiwarter, X. Yan, A. Bleeker and M. A. Sutton, *Environ. Res. Lett.*, 2016, **11**, 120205.
- J. N. Galloway, J. D. Aber, J. W. Erisman, S. P. Seitzinger, R. W. Howarth, E. B. Cowling and B. J. Cosby, *BioScience*, 2003, **53**, 341–356.
- H. Shibata, J. N. Galloway, A. M. Leach, L. R. Cattaneo, L. Cattell Noll, J. W. Erisman, B. Gu, X. Liang, K. Hayashi, L. Ma, T. Dalgaard, M. Graversgaard, D. Chen, C. M. Nansai, J. Shindo, K. Matsubae, A. Oita, M. C. Su, S. I. Mishima and A. Bleeker, *Ambio*, 2017, **46**, 129–142.
- N. Gruber and J. N. Galloway, *Nature*, 2008, **451**, 293–296.
- J. N. Galloway, A. R. Townsend, J. W. Erisman, M. Bekunda, Z. Cai, J. R. Freney, L. A. Martinelli, S. P. Seitzinger and M. A. Sutton, *Science*, 2008, **320**, 889–892.
- Climate Change 2021: The Physical Science Basis. Contribution of Working Group I to the Sixth Assessment Report of the Intergovernmental Panel on Climate Change.
- K. Hayashi, H. Shibata, A. Oita, K. Nishina, A. Ito, K. Katagiri, J. Shindo and W. Winiwarter, *Environ. Pollut.*, 2021, **286**, 117559.
- X. Zhang, B. B. Ward and D. M. Sigman, *Chem. Rev.*, 2020, **120**, 5308–5351.
- J.-Y. Fang, Q.-Z. Zheng, Y.-Y. Lou, K.-M. Zhao, S.-N. Hu, G. Li, O. Akdim, X.-Y. Huang and S.-G. Sun, *Nat. Commun.*, 2022, **13**, 7899.
- Y. Liu, X. Zhang and J. Wang, *Chemosphere*, 2022, **291**, 132728.
- S. Xiang, Y. Liu, G. Zhang, R. Ruan, Y. Wang, X. Wu, H. Zheng, Q. Zhang and L. Cao, *World J. Microbiol. Biotechnol.*, 2020, **36**, 144.
- Council of the European Union, Euro 7, 16960/1/23 REV 1, 2023.
- R. M. Heck and R. J. Farrauto, *Appl. Catal., A*, 2001, **221**, 443–457.
- S. Rood, S. Eslava, A. Manigrasso and C. Bannister, *Proc. Inst. Mech. Eng., Part D*, 2020, **234**, 936–949.
- J. Wang, H. Chen, Z. Hu, M. Yao and Y. Li, *Catal. Rev.*, 2015, **57**, 79–144.
- S. K. Hoekman, *SAE Int. J. Fuels Lubr.*, 2020, **13**, 79–98.
- T. Nagasawa, A. Kobayashi, S. Sato, H. Kosaka, K. Kim, H. M. You, K. Hanamura, A. Terada and T. Mishima, *Chem. Eng. J.*, 2023, **453**, 139937.
- H. M. You, T. Nagasawa, J. W. Lee, H. Kwon and K. Kim, *Appl. Surf. Sci.*, 2024, **648**, 159045.
- K. Sato, H. Tomonaga, T. Yamamoto, S. Matsumura, N. D. B. Zulkifli, T. Ishimoto, M. Koyama, K. Kusada, H. Kobayashi, H. Kitagawa and K. Nagaoka, *Sci. Rep.*, 2016, **6**, 28265.
- K. Kusada, D. Wu, Y. Nanba, M. Koyama, T. Yamamoto, X. Q. Tran, T. Toriyama, S. Matsumura, A. Ito, K. Sato, K. Nagaoka, O. Seo, C. Song, Y. Chen, N. Palina, L. S. R. Kumara, S. Hiroi, O. Sakata, S. Kawaguchi, Y. Kubota and H. Kitagawa, *Adv. Mater.*, 2021, **33**, 2005206.
- N. Zhang, C. Ye, H. Yan, L. Li, H. He, D. Wang and Y. Li, *Nano Res.*, 2020, **13**, 3165–3182.
- L. Nie, D. Mei, H. Xiong, B. Peng, Z. Ren, X. I. P. Hernandez, A. DeLaRiva, M. Wang, M. H. Engelhard, L. Kovarik, A. K. Datye and Y. Wang, *Science*, 2017, **358**, 1419–1423.
- J. Tian, K. Khivantsev, Y. Lu, S. Xue, Z. Zhang, J. Szanyi and Y. Wang, *ChemCatChem*, 2024, **16**, e202301227.
- K. Khivantsev, C. G. Vargas, J. Tian, L. Kovarik, N. R. Jaegers, J. Szanyi and Y. Wang, *Angew. Chem., Int. Ed.*, 2021, **60**, 391–398.
- K. Khivantsev, N. R. Jaegers, H. A. Aleksandrov, I. Song, X. I. Pereira-Hernandez, M. H. Engelhard, J. Tian, L. Chen, D. Motta Meira, L. Kovarik, G. N. Vayssilov, Y. Wang and J. Szanyi, *J. Am. Chem. Soc.*, 2023, **145**, 5029–5040.
- Z. Tan, M. Haneida, H. Kitagawa and B. Huang, *Angew. Chem., Int. Ed.*, 2022, **61**, e202202588.
- X. Zhou, K. Han, K. Li, J. Pan, X. Wang, W. Shi, S. Song and H. Zhang, *Adv. Mater.*, 2022, **34**, 2201859.
- H. Asakura, M. Kirihaara, T. Iijima, S. Hosokawa, S. Kikkawa, K. Teramura and T. Tanaka, *Ind. Eng. Chem. Res.*, 2020, **59**, 19907–19917.
- S. Schemme, R. C. Samsun, R. Peters and D. Stolten, *Fuel*, 2017, **205**, 198–221.
- N. Hooftman, M. Messagie, J. Van Mierlo and T. Coosemans, *Renewable Sustainable Energy Rev.*, 2018, **86**, 1–21.
- S. A. Yashnik, *Catal. Ind.*, 2022, **14**, 283–297.
- N. Takahashi, H. Shinjoh, T. Iijima, T. Suzuki, K. Yamazaki, K. Yokota, H. Suzuki, N. Miyoshi, S. Matsumoto, T. Tanizawa, T. Tanaka, S. Tateishi and K. Kasahara, *Catal. Today*, 1996, **27**, 63–69.
- W. S. Epling, L. E. Campbell, A. Yezerets, N. W. Currier and J. E. Parks, *Catal. Rev.: Sci. Eng.*, 2004, **46**, 163–245.
- S. Matsumoto, *Catal. Today*, 2004, **90**, 183–190.
- S. Roy and A. Baiker, *Chem. Rev.*, 2009, **109**, 4054–4091.
- H. Abdulhamid, E. Fridell and M. Skoglundh, *Top. Catal.*, 2004, **30**, 161–168.
- Z. Liu and J. A. Anderson, *J. Catal.*, 2004, **224**, 18–27.



- 41 N. W. Cant, I. O. Y. Liu and M. J. Patterson, *J. Catal.*, 2006, **243**, 309–317.
- 42 L. Olsson, H. Persson, E. Fridell, M. Skoglundh and B. Andersson, *J. Phys. Chem. B*, 2001, **105**, 6895–6906.
- 43 A. Scotti, I. Nova, E. Tronconi, L. Castoldi, L. Lietti and P. Forzatti, *Ind. Eng. Chem. Res.*, 2004, **43**, 4522–4534.
- 44 I. Nova, L. Lietti and P. Forzatti, *Catal. Today*, 2008, **136**, 128–135.
- 45 M. Machida, D. Kurogi and T. Kijima, *J. Phys. Chem. B*, 2003, **107**, 196–202.
- 46 L. Xu and R. W. McCabe, *Catal. Today*, 2012, **184**, 83–94.
- 47 I. Heo, Y. W. You, J. H. Lee, S. J. Schmiege, D. Y. Yoon and C. H. Kim, *Environ. Sci. Technol.*, 2020, **54**, 8344–8351.
- 48 M. Weibel, N. Waldbüßer, R. Wunsch, D. Chatterjee, B. Bandl-Konrad and B. Krutzsch, *Top. Catal.*, 2009, **52**, 1702–1708.
- 49 L. Castoldi, R. Bonzi, L. Lietti, P. Forzatti, S. Morandi, G. Ghiotti and S. Dzwigaj, *J. Catal.*, 2011, **282**, 128–144.
- 50 S. Schönebaum, J. Dornseiffer, P. Mauermann, B. Wolkenar, S. Sterlepper, E. Wessel, R. Iskandar, J. Mayer, T. E. Weirich, S. Pischinger, O. Guillon and U. Simon, *ChemCatChem*, 2021, **13**, 1787–1805.
- 51 M. Pei, Y. Fan, Y. Li, Y. Huang, H. Xu, J. Wang and Y. Chen, *J. Energy Inst.*, 2024, **114**, 101646.
- 52 J. A. Onrubia-Calvo, B. Pereda-Ayo and J. R. González-Velasco, *Catalysis*, 2020, **10**, 208.
- 53 J. Gao, G. Tian and A. Sornioti, *Energy Sci. Eng.*, 2019, **7**, 2383–2397.
- 54 D. V. Velmurugan, T. McKelvey and J. O. Olsson, *IFAC-PapersOnLine*, 2021, **54**, 526–533.
- 55 K. Kasahara and M. Iwamoto, *Handbook of Environmental Catalyst*, NTS Co. Ltd., Japan, 2001.
- 56 T. Souliotis, G. Koltsakis and Z. Samaras, *Catalysts*, 2021, **11**, 539.
- 57 R. F. Horng and H. M. Chou, *Proc. Inst. Mech. Eng., Part D*, 2003, **217**, 183–191.
- 58 W. Xu, J. Cai, J. Zhou, Z. You, Z. Su, N. Shi and Y. Ou, *Energy Technol.*, 2016, **4**, 856–863.
- 59 C. Yu, Y. Yi, J. Zhou and W. Xu, *Inorg. Chem. Front.*, 2023, **10**, 3808–3820.
- 60 C. Yu, T. Pan, X. Zhu, Q. Peng, Y. Yi, J. Zhou and W. Xu, *Sep. Purif. Technol.*, 2023, **322**, 124281.
- 61 W. Xu, J. Zhou, Z. You, Y. Luo and Y. Ou, *ChemCatChem*, 2015, **7**, 450–458.
- 62 B. Yuan, Z. Qian, Z. Zhang, L. Fu, S. Pan, R. Hao and Y. Zhao, *J. Environ. Sci.*, 2022, **120**, 144–157.
- 63 L. Bo and S. Sun, *Front. Chem. Sci. Eng.*, 2019, **13**, 385–392.
- 64 V. Palma, D. Barba, M. Cortese, M. Martino, S. Renda and E. Meloni, *Catalysts*, 2020, **10**, 246.
- 65 H. H. Kim, *Plasma Processes Polym.*, 2004, **1**, 91–110.
- 66 R. Gholami, C. E. Stere, A. Goguet and C. Hardacre, *Philos. Trans. R. Soc., A*, 2018, **376**, 20170054.
- 67 C. Shi, Z.-S. Zhang, M. Crocker, L. Xu, C.-Y. Wang, C. Au and A.-M. Zhu, *Catal. Today*, 2013, **211**, 96–103.
- 68 Z.-S. Zhang, M. Crocker, B.-B. Chen, Z.-F. Bai, X.-K. Wang and C. Shi, *Catal. Today*, 2015, **256**, 115–123.
- 69 Z.-S. Zhang, M. Crocker, B.-B. Chen, X.-K. Wang, Z.-F. Bai and C. Shi, *Catal. Today*, 2015, **258**, 386–395.
- 70 Z. Bai, Z. Zhang, B. Chen, Q. Zhao, M. Crocker and C. Shi, *Chem. Eng. J.*, 2017, **314**, 688–699.
- 71 D. B. Nguyen, N. Matyakubov, S. Saud, I. Heo, S.-J. Kim, Y. J. Kim, J. H. Lee and Y. S. Mok, *Environ. Sci. Technol.*, 2021, **55**, 6386–6396.
- 72 Y. Sekine and R. Manabe, *Faraday Discuss.*, 2021, **229**, 341–358.
- 73 Y. Hisai, Q. Ma, T. Qureshy, T. Watanabe, T. Higo, T. Norby and Y. Sekine, *Chem. Commun.*, 2021, **57**, 5737–5749.
- 74 Y. Sekine, *Faraday Discuss.*, 2023, **243**, 179–197.
- 75 Y. Omori, A. Shigemoto, K. Sugihara, T. Higo, T. Uenishi and Y. Sekine, *Catal. Sci. Technol.*, 2021, **11**, 4008–4011.
- 76 A. Shigemoto, T. Higo, Y. Narita, S. Yamazoe, T. Uenishi and Y. Sekine, *Catal. Sci. Technol.*, 2022, **12**, 4450–4455.
- 77 R. Burch, J. P. Breen and F. C. Meunier, *Appl. Catal., B*, 2002, **39**, 283–303.
- 78 T. Higo, K. Ueno, Y. Omori, H. Tsuchiya, S. Ogo, S. Hirose, H. Mikami and Y. Sekine, *RSC Adv.*, 2019, **9**, 22721–22728.
- 79 A. Shigemoto, Y. Inoda, C. Ukai, T. Higo, K. Oka and Y. Sekine, *Chem. Commun.*, 2024, **60**, 1563–1566.
- 80 P. Kočí, F. Plát, J. Štěpánek, Š. Bártová, M. Marek, M. Kubiček, V. Schmeißer, D. Chatterjee and M. Weibel, *Catal. Today*, 2009, **147**, S257–S264.
- 81 N. Maeda, A. Urakawa and A. Baiker, *J. Phys. Chem. C*, 2009, **113**, 16724–16735.
- 82 J. C. Martínez-Munuera, J. A. Giménez-Mañogil, R. Matarrese, L. Castoldi and A. García-García, *Appl. Sci.*, 2021, **11**, 5700.
- 83 R. Inagaki, R. Manabe, Y. Hisai, Y. Kamite, T. Yabe, S. Ogo and Y. Sekine, *Int. J. Hydrogen Energy*, 2018, **43**, 14310–14318.
- 84 M. Torimoto, S. Ogo, Y. Hisai, N. Nakano, A. Takahashi, Q. Ma, J. G. Seo, H. Tsuneki, T. Norby and Y. Sekine, *RSC Adv.*, 2020, **10**, 26418–26424.
- 85 K. Murakami, Y. Tanaka, R. Sakai, Y. Hisai, S. Hayashi, Y. Mizutani, T. Higo, S. Ogo, J. G. Seo, H. Tsuneki and Y. Sekine, *Chem. Commun.*, 2020, **56**, 3365–3368.
- 86 Z. Zhuang, B. Guan, J. Chen, C. Zheng, J. Zhou, T. Su, Y. Chen, C. Zhu, X. Hu, S. Zhao, J. Guo, H. Dang, Y. Zhang, Y. Yuan, C. Yi, C. Xu, B. Xu, W. Zeng, Y. Li, K. Shi, Y. He, Z. Wei and Z. Huang, *Chem. Eng. J.*, 2024, **486**, 150374.
- 87 M. Konsolakis, *ACS Catal.*, 2015, **5**, 6397–6421.
- 88 X. Wu, J. Du, Y. Gao, H. Wang, C. Zhang, R. Zhang, H. He, G. Lu and Z. Wu, *Chem. Soc. Rev.*, 2024, **53**, 8379–8423.
- 89 E. R. S. Winter, *J. Catal.*, 1974, **34**, 431–439.
- 90 F. Kapteijn, J. Rodríguez-Mirasol and J. A. Moulijn, *Appl. Catal., B*, 1996, **9**, 25–64.
- 91 T. Yamashita and A. Vannice, *J. Catal.*, 1996, **161**, 254–262.
- 92 H. Dandl and G. Emig, *Appl. Catal., A*, 1998, **168**, 261–268.
- 93 E. V. Kondratenko and J. Pérez-Ramírez, *Catal. Lett.*, 2003, **91**, 211–216.
- 94 S. Parres-Escapuz, I. Such-Basañez, M. J. Illán-Gómez, C. Salinas-Martínez de Lecea and A. Bueno-López, *J. Catal.*, 2010, **276**, 390–401.
- 95 P. J. Smeets, M. H. Groothaert, R. M. van Teeffelen, H. Leeman, E. J. M. Hensen and R. A. Schoonheydt, *J. Catal.*, 2007, **245**, 358–368.
- 96 A. Wang, Y. Wang, E. D. Walter, R. K. Kukkadapu, Y. Guo, G. Lu, R. S. Weber, Y. Wang, C. H. F. Peden and F. Gao, *J. Catal.*, 2018, **358**, 199–210.
- 97 J. Arenas-Alatorre, A. Gómez-Cortés, M. Avalos-Borja and G. Díaz, *J. Phys. Chem. B*, 2005, **109**, 2371–2376.
- 98 K. Pacultová, L. Obalová, F. Kovanda and K. Jiráťová, *Catal. Today*, 2008, **137**, 385–389.
- 99 M. Konsolakis, I. V. Yentekakis, G. Pekridis, N. Kaklidis, A. C. Psarras and G. E. Marnellos, *Appl. Catal., B*, 2013, **138–139**, 191–198.
- 100 M. Konsolakis, C. Drosou and I. V. Yentekakis, *Appl. Catal., B*, 2012, **123–124**, 405–413.
- 101 Y. Vadikkeettil, Y. Subramaniam, R. Murugan, P. V. Ananthapadmanabhan, J. Mostaghimi, L. Pershin, C. Batiot-Dupeyrat and Y. Kobayashi, *Renewable Sustainable Energy Rev.*, 2022, **161**, 112343.
- 102 X. Tan, H. Chen, L. Shi, Q. Lu, S. Qi, C. Yi and B. Yang, *Catal. Lett.*, 2023, **153**, 3724–3733.
- 103 J. O. Jo, Q. H. Trinh, S. H. Kim and Y. S. Mok, *Catal. Today*, 2018, **310**, 42–48.
- 104 L. S. Ko, Y. S. Chen, K. L. Pan and M. B. Chang, *Catal. Commun.*, 2023, **177**, 106666.
- 105 O. Muccioli, E. Meloni, S. Renda, M. Martino, F. Brandani, P. Pullumbi and V. Palma, *Processes*, 2023, **11**, 1511.
- 106 E. Meloni, M. Martino, A. Ricca and V. Palma, *Int. J. Hydrogen Energy*, 2021, **46**, 13729–13747.
- 107 A. Shigemoto, T. Higo, C. Ukai, Y. Inoda, K. Mitarai and Y. Sekine, *Catal. Sci. Technol.*, 2024, **14**, 4471–4478.
- 108 M.-J. Kim, H. J. Kim, S.-J. Lee, I.-S. Ryu, H. C. Yoon, K. B. Lee and S. G. Jeon, *Catal. Commun.*, 2019, **130**, 105764.
- 109 A. Suda, K. Yamamura, Y. Ukyo, T. Sasaki, H. Sobukawa, T. Tanabe, Y. Nagai and M. Sugiura, *J. Ceram. Soc. Jpn.*, 2004, **112**, 581–585.
- 110 S. Ogo, H. Nakatsubo, K. Iwasaki, A. Sato, K. Murakami, T. Yabe, A. Ishikawa, H. Nakai and Y. Sekine, *J. Phys. Chem. C*, 2018, **122**, 2089–2096.
- 111 K. Takise, A. Sato, K. Muraguchi, S. Ogo and Y. Sekine, *Appl. Catal., A*, 2019, **573**, 56–63.
- 112 C. Moreau, A. Caravaca, P. Vernoux and S. Gil, *ChemCatChem*, 2020, **12**, 3042–3049.



- 113 G. S. Zafiris and R. J. Gorte, *J. Catal.*, 1993, **139**, 561–567.
- 114 K. Yamashita, Z. Liu, K. Iyoki, C. T. Chen, S. Miyagi, Y. Yanaba, Y. Yamauchi, T. Okubo and T. Wakihara, *Chem. Commun.*, 2021, **57**, 1312–1315.
- 115 T. Wu, Y. Shen, L. Feng, Z. Tang and D. Zhang, *J. Chem. Eng. Data*, 2019, **64**, 3473–3482.
- 116 Y. Peng, F. Zhang, C. Xu, Q. Xiao, Y. Zhong and W. Zhu, *J. Chem. Eng. Data*, 2009, **54**, 3079–3081.
- 117 K. Severin, *Chem. Soc. Rev.*, 2015, **44**, 6375–6386.
- 118 F. Le Vaillant, A. M. Calbet, S. González-Pelayo, E. J. Reijerse, S. Ni, J. Busch and J. Cornella, *Nature*, 2022, **604**, 677–683.
- 119 J. Yang, B. Du, J. Liu, R. Krishna, F. Zhang, W. Zhou, Y. Wang, J. Li and B. Chen, *Chem. Commun.*, 2018, **54**, 14061–14064.
- 120 B. Yue, X. Lian, S. Liu, G. Wu, J. Xu and L. Li, *Chem. Eng. J.*, 2023, **462**, 142300.
- 121 S. Hiraki, H. Baba, I. Kobayashi, A. Oda, T. Ohkubo, Y. Ikemoto, T. Moriwaki and Y. Kuroda, *Chem. Commun.*, 2024, **60**, 4597–4600.
- 122 E. Meloni, M. Martino, M. Pierro, P. Pullumbi, F. Brandani and V. Palma, *Energies*, 2022, **15**, 4119.
- 123 Q. H. Trinh, S. H. Kim and Y. S. Mok, *Chem. Eng. J.*, 2016, **302**, 12–22.
- 124 Y. Jing, C. He, L. Wan, J. Tong, J. Zhang, S. Mine, N. Zhang, Y. Kageyama, H. Inomata, K. Shimizu and T. Toyao, *ACS ES&T Eng.*, 2024, DOI: [10.1021/acsestengg.4c00560](https://doi.org/10.1021/acsestengg.4c00560).
- 125 USDRIVE, Aftertreatment Protocols for Catalyst Characterization and Performance Evaluation: Low-Temperature Oxidation Catalyst Test Protocol, 2015.

